ISSN: 2454-9940

INTERNATIONAL JOURNAL OF APPLIED SCIENCE ENGINEERING AND MANAGEMENT

E-Mail :
editor.ijasem@gmail.com
editor@ijasem.org

www.ijasem.org

INTERNATIONAL JOURNAL OF APPLIED SCIENCE ENGINEERING AND MANAGEMENT

ISSN2454-9940

www.ijasem.org

Vol 17, Issue 1, 2023

Optimizing PEEK impact strength through multi-objective FDM 3D printing

Dr. C. Prabha, Dr. R. Suresh Kumar, Mr. P. Vineeth kumar, Mr. V. Prakash

Professor [2] Associate Professor [1], Assistant Professor [3,4]

cprabha@actechnology.in, sureshkumar.r@actechnology.in, vineethkumar.p@actechnology.in, vprakash@actechnology.in

Department of MECHANICAL ENGINEERING, Arjun College of Technology, Thamaraikulam, Coimbatore-Pollachi Highway, Coimbatore, Tamilnadu-642 120

1.0 INTRODUCTION

Design flexibility, lower material utilisation, and near net shape production (NNSP) are just a few of the benefits that additive manufacturing (AM) provides over traditional manufacturing. Thanks to its simplicity, cost, and many applications in prototyping, engineering, and education, fused filament fabrication (FFF), also known as fused deposition modelling (FDM), has become a popular AM process among many others [1, 2]. In comparison to other methods, FDM has lower system costs and shorter build times because to its layer-by-layer method of employing melted filament, which allows for efficient item construction with minimum waste formation. Form, function, and fitness are all factors that designers take into account while creating 3D printed products using FDM. The development of high-performance polymers has made it more difficult to achieve desirable mechanical properties through FDM. It is especially crucial to mechanically test high-grade polymers such as Polyether ether ketone (PEEK), Polyetherketoneketone (PEKK), and Polyethylenimine (PEI) that serve as metal replacements [3, 4]. Numerous biomedical therapies have made extensive use of PEEK and its variants. These include maxillofacial surgery, orthopaedic surgeries, dental implants, and other similar procedures. Its high strength-to-weight ratio and long service life have also made it a favourite among many manufacturers [5]. Engineers may test the strength, durability, performance, and structural integrity of a component by putting it through a series of mechanical stresses, including compression, bending, torsion, and tension. By doing so, they are able to pinpoint any restrictions or shortcomings and make educated choices to enhance designs appropriately. Improving mechanical properties like tensile, compression, and flexural strengths, as well as overall part performance and durability, has been the subject of several studies [6–8] that have concentrated on optimising FDM-AM process parameters. These parameters include layer thickness, raster angle, print speed, nozzle temperature, infill patterns, and density. In order to increase the use of 3D printed components in different sectors, it is crucial to comprehend and enhance these mechanical characteristics.

.

INTERNATIONAL JOURNAL OF APPLIED SCIENCE ENGINEERING AND MANAGEMENT

ISSN2454-9940

www.ijasem.org

Vol 17, Issue 1, 2023

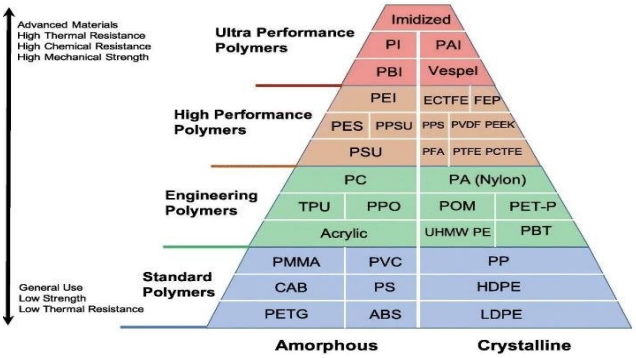

Figure 1. Classification of polymers [9]

Focussing on PEEK, a high-performance thermosetting polymer, this research aims to assess the impact behaviour of 3D-printed components made from high-performance polymers. While several studies have looked at how different process factors affect 3D printed PEEK components, the correlation between process parameters, build time, and impact strength has received comparatively less attention. To better understand how filler content affects mechanical properties and tribological properties of PEEK composites, Zhang et al. (2004) investigated this topic [10]. Wu et al. (2014) examined the effect of printing settings on thermal deformation and dimensional accuracy in 3D printed PEEK. They discovered that although the printing technique achieved excellent precision, it was susceptible to distortion when subjected to high temperatures [11]. Higher printing and chamber temperatures enhanced crystallinity and strength, but slower cooling rates improved crystallisation and mechanical performance, according to Yang et al. (2017), who studied the effects of thermal processing parameters on the mechanical characteristics and crystallinity of PEEK [12]. In their 2017 study, Berretta et al. compared FDM-fabricated CNT-PEEK composites to pure PEEK in terms of mechanical qualities and thermal behaviour, and they found that the addition of carbon nano tubes (CNTs) increased mechanical capabilities but decreased thermal stability [13]. Printing parameters had a major influence on the mechanical strength of 3D printed PEEK components, as shown by Rinaldi et al. (2018). Printing temperatures had a positive effect on mechanical characteristics, whereas raster angle and layer height had a negative effect [14]. Deng et al. (2018) investigated the best temperature, speed, and infill density settings for FDM printing of PEEK in order to improve its mechanical characteristics [15]. Print orientation, layer thickness, and the impact of post-processing on mechanical behaviour and surface quality were examined in Arif et al.'s (2018) study of biocompatible PEEK qualities [16]. Subsequently, in 2019, Saja et al. explored PEEK's mechanical characteristics in an effort to determine its suitability as a denture material [17]. According to Wang et al. (2019), PEEK surface quality was enhanced with higher printing temperatures and lower printing rates, while flaws and degradation were produced by excessive temperatures [18]. Concurrently, Li et al. (2019) examined the effects of building orientation, fibre content, and fibre length on the flexural characteristics and fracture behaviour of CF/PEEK composites [19]. Adding multi-walled carbon nanotubes (MWCNTs) to PEEK increased its impact strength, according to Yingshuang et al. (2019) [20]. In addition, a 2019 research by Haijun et al. studied the impact strength of 3D printed PEEK. The study primarily focused on evaluating PEEK's resistance to impact pressures, which provided more insights into its mechanical performance and indicated practical prospective uses [21]. A study conducted by Singh et al. (2019) investigated the use of 3D printing technology to produce PEEK components for a range of biomedical uses, yielding valuable insights for the medical and healthcare industries [22]. Composite filaments made of PEEK and HA were produced by Zheng et al. (2021), who found that their material had a higher tensile modulus but lower tensile strength than pure PEEK [23]. In the field of 3D printing, there has been little study on the correlation between process parameters, build time, and impact strength as it pertains to high-performance polymers. For the purpose of evaluating production process safety, efficiency, and quality control, it is essential to understand and measure the optimal material impact strength.

So, taking material utilisation and production efficiency into account, this study intends to evaluate the impact behaviour of 3D printed components and investigate the effect of process factors on impact strength, namely print orientation, infill density, and environmental conditions—chamber temperature. An overview of the FDM method using PEEK and pertinent studies on process parameter optimisation are included in the article's arrangement. Detailed descriptions of the experiments, methods, extensive analyses of the data, and discussions of the key results follow, followed by a brief summary and last thoughts on the subject.

2.0 EXPERIMENTAL DETAILS

Figure 2 shows the schematic layout of FDM 3D PEEK printing, where CreatBot F160 PEEK-3D printer (manufacturer: Createbot Inc, China) is used to create the specimens. The 3D printer is equipped with a sizable build volume of (x:160mm, y:160mm, z:200mm) and incorporates a specialised heating system optimised for handling high-grade polymers efficiently.

ISSN2454-9940
www.ijasem.org
Vol 17, Issue 1, 2023

2.1 Setting Parameters

Given the constraints of the research scope, the authors focused on the most critical printing parameters that directly impact the impact strength of thermoplastic polymers. These parameters were carefully selected based on insights gleaned from various previous studies. For the investigation, the author chose to work with PEEK, a high-grade polymer featuring a filament diameter of 1.75 mm. Table 1 outlines the essential properties of PEEK. By systematically studying the influence of specific printing parameters on PEEK's mechanical properties, the aim was to gain valuable insights into enhancing the impact strength of 3D printed PEEK components.

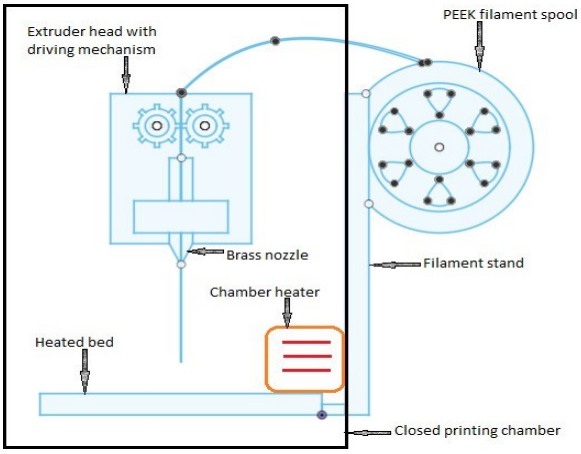

Figure 2. Schematic layout of FFF 3D PEEK printing

2.2 Sample Preparation

A nano polymer adhesive (manufacturer: Visionminer) designed for high-temperature build plate glue was initially used to address the common issue of bottom layer stick-out encountered while handling PEEK in Fused Deposition Modeling (FDM-AM). To further enhance print quality and reduce defects caused by moisture in the PEEK filament, the filament was dried in a filament drier (manufacturer: Creality Inc.) for 2 hours at 60^{0}C, following the recommendations from Cicala et al. (2017) [24]. For the experiment, SolidWorks (2022 edition) was employed to model the printed samples according to ASTM standards (refer to Figure 3). The STL file (*.stl) of the samples was then imported into Simplify3D, a licensed 3D slicing software, to configure print parameters and generate the necessary G-Code for the 3D-printer. To optimise the impact strength (IS) of PEEK, the study considered various print parameters, such as chamber temperature (CT) and build orientation (XY: horizontal, XZ: vertical, refer to Figure 4(a) and (b). Specimens were printed using the optimised parameters for strength [25] which included a layer thickness of 0.01 mm, nozzle temperature of 440 °C, print direction at 0°, while printed with a speed of 15 mm/sec and 0.4 mm brass nozzle [25]. The bed temperature was maintained at 120 °C for printing all specimens used in this research. The impact of print density, along with other selected print parameters on the impact strength of PEEK was investigated through the fabrication of the specimens (refer to Figure 4(c)). Moreover, balancing the strength, weight, and print time, the optimal infill density was determined through iterative testing and adjustments.

Table 1. Properties of PEEK [3]

Properties	Values	Properties	Values
Specific gravity	1.3 gm/cc	Flexural strength	125-128 MPa
Glass transition temperature	143 ^{0}C	Young's modulus	3.7 GPa
Melting point	340 ^{0}C	Operating temperature	250 ^{0}C

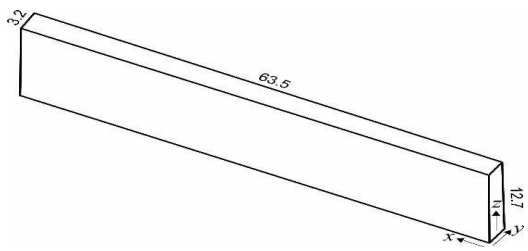

Figure 3. CAD model of the specimen (all dimensions are in mm)

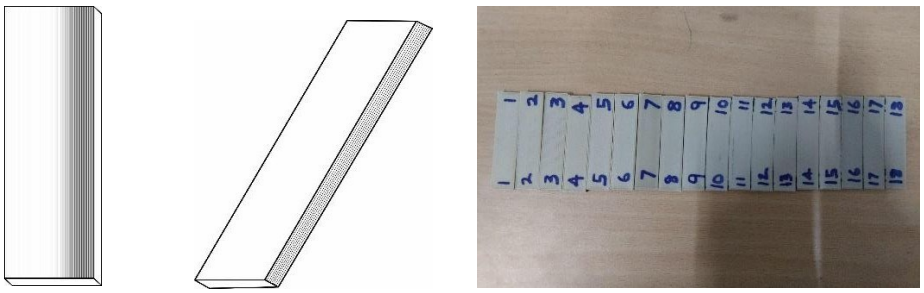

(a) (b) (c)

Figure 4. Representation of: (a) XY-build orientation, (b) XZ-build orientation and (c) Printed impact test specimens

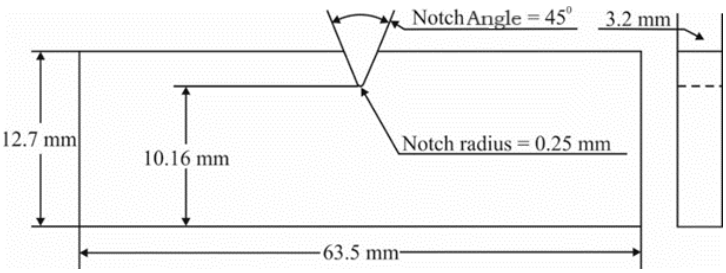

Figure 5. Specification of notched ASTM D256 specimen

2.3 Sample Testing

Subsequently, the printed specimens were notched in accordance with the ASTM standard (see Figure 5) and prepared for the mechanical Izod impact test (see Figure 6). The Izod impact test was conducted using an Izod impact tester (manufacturer: Deepak Polyplast, Unique ID No.: KL/ICT/01, Sl. No.: 2K103074) equipped with a digital impact indicator and a hammer mass of 4260 gms (see Figure 7).

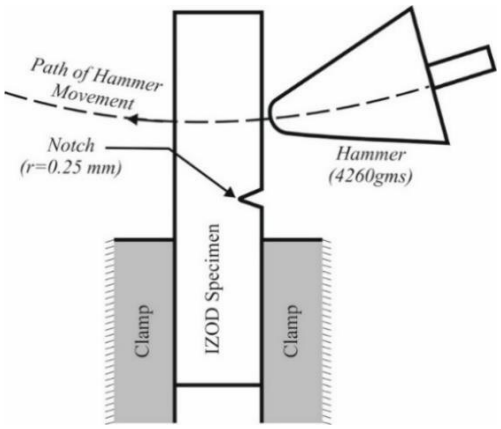

Figure 6. Impact test of ASTM D256 specimen

Figure 7. Izod impact test equipment

ISSN2454-9940
www.ijasem.org
Vol 17, Issue 1, 2023

3.0 METHODOLOGY

The optimization of the 3D printing process involves systematically selecting appropriate process parameter values to achieve specific objectives, where the desired response variable or performance parameter is maximized or minimized. In simpler terms, it's about finding the best combination of settings to achieve the desired outcome in the 3D printed object. In this PEEK material based printing process parameters, namely, print orientation (PO), print density (PDN) and chamber temperature (CT) [in ^{0}C] are considered. In extrusion based 3D printing process, the mentioned process parameters are highly discussed in the earlier published articles as mentioned in the introduction section. Now, three response variable or performance variables, namely, print time (PT) [in mins], impact strength (IS) [in kJ/m^2] and material used (MU) [in gms] are considered in this article. In the manufacturing sector, production time is a vital parameter to measure the efficiency of the manufacturing process along with the product quality. On the other hand, in case of 3D printing process, impact strength is one of the important parameters for measuring the print quality. Along with these response parameters, material utilization indicator related to printing cost, is also considered as one of the important response variable. This research initially uses analysis of variance (ANOVA) method for finding the individual process parameters impact on the selected response variable. Next correlation analysis has been used to know the association between the process parameters and the response variables. The ANOVA and Correlation analysis indicates a proper explanation of the relationship between them. Then two different modified Taguchi methods, namely, Taguchi and Composite Desirability Taguchi (TOPSIS), are used to optimize the method and the final results are compared with mix Taguchi method for result comparison and at the end a Regression equation is derived for estimating the impact strengthof printed object for PEEK.

3.1 Data Generation

The initial data generation has been done through conducting lab experiments. In this article the data for the analysis has been generated based on the orthogonal array L18, which is a schema for performing experiments [26]. Here the L18 orthogonal array is selected as the number of process parameters are three with a mixed number of levels. The detailed level information for various input parameters including output parameters used in this article has been provided in Table 2. Also the parameters, which are kept constant during the printing process, are provided in the same Table 2.

Table 2. Details of printing parameters

Input Parameter(s)				Output Parameter(s)
Level (s)	Level 1	Level 2	Level 3	
Print Orientation (PO)	XY	XZ	-	Impact Strength (IS)
Print Density (PDN)	High (100%)	Medium (90%)	Low (80%)	Print Time (PT)
Chamber Temperature (CT)	70° C	60° C	50° C	Material Utilization (MU)
Other setting print parameters, which are kept constant				
Nozzle temperature	440 ^{0}C	Print speed	15 mm/sec	
Layer height	0.01 mm	Print direction	0^0	

The orthogonal array with the response values is provided in Table 3. In this table aforementioned three process parameters levels along with the response values, which are obtained through lab testing are provided. This data set is further used for all kind of data analysis process for performing correlation analysis, analysis of variance, process optimization and regression analysis.

Table 3. L18 OA data for analysis

TN	PO	PDN (%)	CT (^{0}C)	PT (mins)	IS (kJ/m^2)	MU (gms)
1	XY	80	50	84	74.03	3.08
2	XY	80	60	84	75.51	3.08
3	XY	80	70	84	75.88	3.08
4	XY	90	50	89	117.59	3.27
5	XY	90	60	89	91.33	3.27
6	XY	90	70	89	100.51	3.27
7	XY	100	50	98	112.48	3.64
8	XY	100	60	98	81.61	3.64
9	XY	100	70	98	96.53	3.64
10	XZ	80	50	84	65.25	3.08
11	XZ	80	60	84	71.79	3.08
12	XZ	80	70	84	55.98	3.08

ISSN2454-9940
www.ijasem.org
Vol 17, Issue 1, 2023

Table 3. (cont.)

TN	PO	PDN (%)	CT (^{0}C)	PT (mins)	IS (kJ/m^2)	MU (gms)
13	XZ	90	50	89	86.98	3.27
14	XZ	90	60	89	72.63	3.27
15	XZ	90	70	89	99.78	3.27
16	XZ	100	50	98	230.4	3.64
17	XZ	100	60	98	224.13	3.64
18	XZ	100	70	98	225.49	3.64

*TN=Treatment No.

3.2 Analysis of variance (ANOVA)

Analysis of variance is a process where the variances in response variables are analyzed to understand the contribution of each process parameter. The ANOVA has been conducted for each response variable and tabulated the summary of the analysis in Tables 4 through 6 [26]. The important statistics can be found in the table which are useful for describing the phenomenon.

Table 4. Analysis of variance for impact strength

Source	df	Adj SS	Adj MS	F Value	P Value	VIF
Regression	3	30733.4	10244.5	6.06	0.007	
PDN	1	25410.4	25410.4	15.04	0.002	1
CT	1	88.3	88.3	0.05	0.822	1
PO	1	5234.7	5234.7	3.10	0.100	1
Error	14	23648.2	1689.2			
Total	17	54381.6				

Table 5. Analysis of variance for print time

Source	df	Adj SS	Adj MS	F	p	VIF
Regression	3	588.0	196.000	171.50	0.00	
PDN	1	588.0	588.000	514.50	0.00	1
CT	1	0.0	0.000	0.00	1.00	1
PO	1	0.0	0.000	0.00	1.00	1
Error	14	16.0	1.143			
Total	17	604.0				

Table 6. Analysis of variance for material used

Source	df	Adj SS	Adj MS	F	p	VIF
Regression	3	0.9408	0.3136	135.51	0.00	
PDN	1	0.9408	0.9408	406.52	0.00	1
CT	1	0.000	0.0000	0.00	1.00	1
PO	1	0.000	0.0000	0.00	1.00	1
Error	14	0.0324	0.002314			
Total	17	0.9732				

According to the Tables 4 through 6, the contribution of PDN in variance for all response variables is highest. In caseof impact strength, the second highest contributor in variance is print orientation (PO). Similarly based on the F value andp value it can be stated that the (PDN) has a significant impact on the response variables.

3.3 Pearson Correlation

A correlation analysis has been conducted to know the association between different types of variables before processoptimization. Pearson correlation is a method for finding the statistical association between two variables. This basicallyis the ratio of covariance and product of standard deviation. The correlation coefficient provides useful information how the two variables behaves to each other according to the collected data. The expression for calculating the Pearson correlation coefficient (r_p) is provided in Eq. (1) [27]. The calculated correlation coefficients are provided in Table 7.

$$r_p = \frac{\sigma_{x,y}}{\sigma_x \sigma_y} \tag{1}$$

where, $\sigma_{x,y}$ is indicating the covarience of two variables x and y, σ_x and σ_y are the standard deviation of x and y.

Table 7. Correlation analysis summary

	PDN	CT	PT	IS	MU
PDN	1.000				
CT	0.000	1.000			
PT	0.987**	0.000	1.000		
IS	0.684**	-0.040	0.704**	1.000	
MU	0.983**	0.000	1.000**	0.705**	1.000
** indicates the 95% confidence interval					

According to the data, material utilization (MU) and print time (PT) has full positive significant correlation. Similarly, impact strength (IS) and MU have high significant positive correlation (0.705**). The impact strength is high positively correlated to print time (0.704**). As per the correlation values, if only material utilization is considered in analysis then the print time will be automatically taken care off. So, accordingly further in the optimization of process only MU and IS are considered. The correlation analysis also indicates that which process parameters out of the selected three process parameter need to be given importance while optimizing the process. The correlation analysis indicates the print density have high positive correlation on the IS, MU and PT. So, print density is an important parameter while optimizing the process in the present scenario.

3.4 Taguchi's Design of Experiment

Taguchi's design of experiment (DOE) is an optimization method, which considers the impact of the levels of the process parameters on the response value. This method is a very popular method of optimization as it considers the loss function for finding the right combination of process parameter levels to generate the optimal value of response. The twoconcepts for such optimization are Smaller-the-better and Larger-the-better. The signal to noise ratio for smaller the better(SNR_s) and larger the better (SNR_L) calculations for the two cases are represented with Eqs. (2) and (3) [26].

$$SNR_s = -10 \log \log \left(\frac{1}{n} \sum_{i=1}^{n} y_i^2\right) \tag{2}$$

$$SNR_L = -10 \log \log \left(\frac{1}{n} \sum_{i=1}^{n} \frac{1}{y_i^2}\right) \tag{3}$$

The Taguchi method is applied to optimize individual response variables. The main effect and signal to noise effect has been observed and the effects are provided in Tables 8 through 10.

Table 8. Main effect of signal to noise ratio and mean value for impact strength

	Signal to noise ratio			Mean		
Levels	PO	PDN	CT	PO	PDN	CT
1	39.13	36.82	40.36	91.72	69.74	114.46
2	40.63	39.44	39.39	125.83	94.80	102.83
3		43.38	39.89		161.77	109.03
Delta	1.50	6.56	0.96	34.11	92.03	11.62
Rank	2	1	3	2	1	3

Table 9. Main effect of signal to noise ratio and mean value for print time

	Signal to noise ratio			Mean		
Levels	PO	PDN	CT	PO	PDN	CT
1	-39.10	-38.49	-39.10	90.33	84.00	90.33
2	-39.10	-38.99	-39.10	90.33	89.00	90.33
3		-39.82	-39.10		98.00	90.33
Delta	0.00	1.34	0.000	0.000	14.00	0.000
Rank	2.5	1	2.5	2.5	1	2.5

Table 10. Main effect of signal to noise ratio and mean value material used

	Signal to noise (S/N) ratio			Mean		
Levels	PO	PDN	CT	PO	PDN	CT
1	-10.428	-9.771	-10.428	3.330	3.080	3.330
2	-10.428	-10.291	-10.428	3.330	3.270	3.330
3		-11.222	-10.428		3.640	3.330
Delta	0.000	1.451	0.000	0.000	0.560	0.000
Rank	2.5	1	2.5	2.5	1	2.5

The data is analysed using the Taguchi DOE for the objective of smaller the better. Here for the three response parameters data analysis has been presented in Tables 6 through 8. In Table 6, 7, and 8 the main effect of signal to noiseratio (S/N) and mean can be observed where the PDN got the highest rank of 1. On the other hand, PO and CT have an equal rank of 2.5 for PT and MU. While, in case of IS, the PO has got rank 2 and CT ranked as 3.

3.5 Technique for Order Preference by TOPSIS based Taguchi

Technique for TOPSIS is a method for selecting the best alternative based on the criteria values [28]. The technique is a well-known multicriteria decision making method and this method is utilized for combining the three response variables into a single variable for applying the Taguchi based response optimization.

Step 1: Prepare the table containing the alternatives and criteria values (x_{ij}). Fix the weight values (w_{ij}) for the criterias.

Step 2: Normalise the criteria values for particular alternatives using Eq. (4).

$$r_{ij} = \frac{x_{ij}}{\sqrt{\sum_{k=1}^{m} x_{kj}^2}} \qquad i = 1,2,3, \dots \dots . n \; ; j = 1,2,3 \dots \dots . . m \tag{4}$$

where n is the number of alternatives and m is the number of criteria.

Step 3: Calculate the weighted normalised values (v_{ij}) for criteria for alternatives based on the Eq. (5).

$$v_{ij} = r_{ij} \times w_{ij} \tag{5}$$

Step 4: Identify the positive ideal solution (A^+) and negative ideal solution (A^-) which are represented with Eqs. (6) and (7).

$$A^+ = \{v_1^+, v_2^+, \dots . . , v_m^+\} \tag{6}$$

$$A^- = \{v_1^-, v_2^-, \dots . . , v_m^-\} \tag{7}$$

Step 5: Calculate the distance (d_{pi}) between every alternative and positive ideal solution using Eq. (8). Similarly, calculate the distance (d_{ni}) between every alternative and negative ideal solution using Eq. (9).

$$d_{pi} = \sqrt{\sum_{j=1}^{m} (v_{ij} - v_j^+)^2} \tag{8}$$

$$d_{ni} = \sqrt{\sum_{j=1}^{m} (v_{ij} - v_j^-)^2} \tag{9}$$

Step 6: Now calculate (C^*) using Eq. (10). The range of value for $0 \leq C^* \leq 1$

$$C^* = \frac{d_{pi}}{d_{pi} + d_{ni}} \tag{10}$$

Here, the lower value of C^* is desired as it indicates a solution nearer to the positive ideal solution. In the proposed methodology this C^* is used as the response variable for Taguchi's design for experiment based optimization. Such an approach of hybridization, where a multicriteria decision making approach is combined with design of experiment can be found in recent literature [29, 30] for combining several objectives.

The 18-treatment condition can be considered as alternatives for the process of the TOPSIS method. The three response variables can be considered as the criteria for the best alternative selection. Two different sets of weight values are considered (0.4,0.3,0.3) and (0.5,0.25,0.25) for IS, PT and MU. The main reason for assigning same weight values to PT and MU is because of the full correlation between them ($r_p = 1.00^{**}$).The TOPSIS scores C^* for these two cases are

ISSN2454-9940
www.ijasem.org
Vol 17, Issue 1, 2023

provided in Figure 8. The intermediate calculation of weighted normalised matrix, distance from positive ideal solution (d_{pi}), distance from negative idle solution (d_{ni}) and TOPSIS score C^* for each alternative has been provided for the two cases with different criteria weights in Table 11 and Table 13 given below. The ANOVA for the two TOPSIS scores are also provided in Table 12 and Table 14. This selection of best alternative using TOPSIS has been conducted for weight values of IS, keeping the other two responses with equal weightage indicates no change in best alternative selection.

Table 11. Weighted normalized alternatives for TOPSIS case 1

	W_{IS}	W_{PT}	W_{MU}			
	0.4	0.3	0.3			
Alternatives	nIS*w	nPT*w	nMU*w	d_{pi}	d_{ni}	C^*
1	0.057270408	0.065618325	0.065243	0.12096952	0.021338	0.850057801
2	0.058415352	0.065618325	0.065243	0.11982458	0.022104	0.844259063
3	0.058701588	0.065618325	0.065243	0.11953834	0.022301	0.842774403
4	0.090968894	0.069524178	0.069268	0.08745106	0.048811	0.641784616
5	0.070653874	0.069524178	0.069268	0.10773214	0.029304	0.786158688
6	0.077755622	0.069524178	0.069268	0.1006407	0.036022	0.736416829
7	0.087015743	0.076554713	0.077106	0.09264002	0.043709	0.67943292
8	0.063134377	0.076554713	0.077106	0.11623084	0.019828	0.854271166
9	0.074676651	0.076554713	0.077106	0.10481256	0.03137	0.769647921
10	0.050478105	0.065618325	0.065243	0.12776182	0.017656	0.878581716
11	0.055537519	0.065618325	0.065243	0.12270241	0.020246	0.85836659
12	0.043306733	0.065618325	0.065243	0.1349332	0.016134	0.893197063
13	0.067288667	0.069524178	0.069268	0.11109292	0.026191	0.809217711
14	0.056187352	0.069524178	0.069268	0.12218136	0.016636	0.880156954
15	0.077190886	0.069524178	0.069268	0.10120456	0.035482	0.74041181
16	0.178239928	0.076554713	0.077106	0.01613447	0.134933	0.106802937
17	0.173389389	0.076554713	0.077106	0.01684782	0.130083	0.114665222
18	0.174441499	0.076554713	0.077106	0.01657556	0.131135	0.112216665

**Note: PIS: [0.065618325,0.178239928,0.065243]; NIS: [0.076554713,0.043306733,0.077106]
W indicates the weight value for particular response variable, n indicates the normalized value.

ISSN2454-9940
www.ijasem.org
Vol 17, Issue 1, 2023

Table 12. Analysis of variance for first case 1

Source (TS1)	df	Adj SS	Adj MS	F	p	VIF
Regression	3	1.03829	0.346096	6.59	0.005	
PDN	1	0.87513	0.875135	16.67	0.001	1.00
CT	1	0.00267	0.002668	0.05	0.825	1.00
PO	1	0.16048	0.160484	3.06	0.102	1.00
Error	14	0.73500	0.052500			
Total	17	1.77328				

Table 13. Weighted normalised alternatives for TOPSIS case 2

	W_{IS}	W_{PT}	W_{MU}			
	0.5	0.25	0.25			
Alternatives	nIS*w	nPT*w	nMU*w	d_{pi}	d_{ni}	C^*
1	0.071588009	0.054681938	0.054369	0.15199633	0.036056	0.808267094
2	0.073019189	0.054681938	0.054369	0.15057261	0.03677	0.803728824
3	0.073376984	0.054681938	0.054369	0.1502167	0.036955	0.802561012
4	0.113711117	0.057936815	0.057723	0.10961715	0.065359	0.626468983
5	0.088317343	0.057936815	0.057723	0.13491151	0.043484	0.756250303
6	0.097194527	0.057936815	0.057723	0.12606454	0.05076	0.71293648
7	0.108769679	0.063795594	0.064255	0.11404908	0.057559	0.664589572
8	0.078917972	0.063795594	0.064255	0.14389688	0.030696	0.824187466
9	0.093345813	0.063795594	0.064255	0.1294707	0.043192	0.749847293
10	0.063097631	0.054681938	0.054369	0.1604452	0.032798	0.83027575
11	0.069421899	0.054681938	0.054369	0.15415142	0.035058	0.814711362
12	0.054133416	0.054681938	0.054369	0.1693701	0.031549	0.842975485
13	0.084110834	0.057936815	0.057723	0.13910505	0.040261	0.775537348
14	0.070234191	0.057936815	0.057723	0.15294396	0.031329	0.829983818
15	0.096488607	0.057936815	0.057723	0.1267679	0.050162	0.716485118
16	0.22279991	0.063795594	0.064255	0.00207354	0.169636	0.012075839
17	0.216736736	0.063795594	0.064255	0.00640794	0.163609	0.037690066
18	0.218051874	0.063795594	0.064255	0.00518106	0.164916	0.030459486

**Note PIS: [0.054681938, 0.22279991, 0.054369]; NIS: [0.063795594,0.054133416,0.064255],
W indicates the weight value for particular response variable, n indicates the normalized value.

Table 14. Analysis of variance for case 2

Source (TS2)	df	Adj SS	Adj MS	F	p	VIF
Regression	3	0.471945	0.157315	6.69	0.005	
PDN	1	0.436419	0.436419	18.55	0.001	1.00
CT	1	0.002183	0.002183	0.09	0.765	1.00
PO	1	0.033344	0.033344	1.42	0.254	1.00
Error	14	0.329298	0.023521			
Total	17	0.801243				

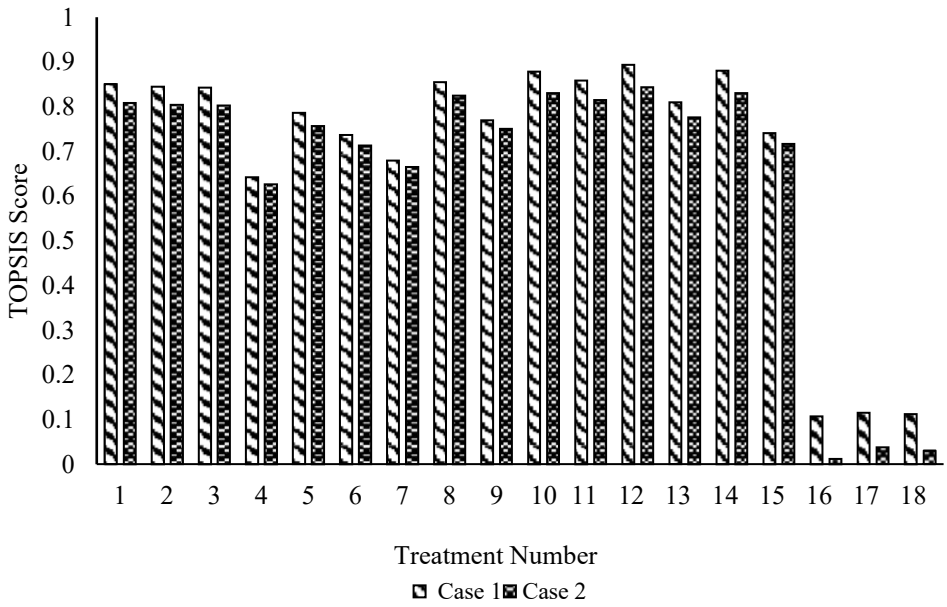

Figure 8. Weighted normalised alternatives for TOPSIS score for two cases

The application of the Taguchi based method on the TOPSIS scores for two cases indicates that the importance of PDN is highest followed by PO and CT. The main effects of signal to noise ratio and mean for both cases are provided inTable 15 and Table 16. The delta values and rank for all process parameters are provided in same tables. The score of $C^*$is used as the response variable for Taguchi design experiment with smaller-the-better approaches. The calculated levels for the three process paramaters are PDN=100%, PO=XZ and CT=50^0C. The details for the results has been provided inresults discussion. So further, the same problem has been solved using composite desirability.

Table 15. Main effect of signal to noise ratios and mean for case 1

	Signal to Noise ratio			Mean		
Levels	PO	PDN	CT	PO	PDN	CT
1	2.218	1.300	5.169	0.7783	0.8612	0.6610
2	7.359	2.360	4.363	0.5993	0.7657	0.7230
3		10.706	4.835		0.4395	0.6824
Delta	5.140	9.406	0.806	0.18885	0.4217	0.0620
Rank	2	1	3	PO	PDN	CT

Table 16. Main effect of signal to noise ratios and mean for case 2 (Smaller is the better)

	Signal to Noise ratio			Mean		
Levels	PO	PDN	CT	PO	PDN	CT
1	2.132	1.047	5.602	0.7867	0.8867	0.6655
2	8.229	2.291	4.720	0.6009	0.7720	0.7284
3		12.203	5.220		0.4228	0.6875
Delta	6.098	11.155	0.883	0.1858	0.4639	0.0629
Rank	2	1	3	2	1	3

3.6 Composite Desirability Based Optimization

The traditional Taguchi analysis can provide the optimal process parameter value for a specific objective, but it has limitation in tackling multiple objectives. Now here two objectives, namely, maximum impact strength and minimum material utilization is considered as there two parameters for optimization problem. The composite desirability, D is calculated based on the Eqs. (11) through (13) [31], whereas desirability function $d_j(Y_j)$ is used to converts the response values $Y_j(x)$, between 0 and 1. The individual desirability values are combined using Eq. (11), which gives the compositedesirability, D.

$$D = (d_1(Y_1) \times d_1(Y_1) \times \ldots\ldots\ldots \times d_k(Y_k))^{\frac{1}{k}} \tag{11}$$

where, 'k' is the number of responses. The desirability for maximization is presented in Eq. (12).

$$d_j(Y_j) = \begin{cases} 0 & if\ Y_j < L_j \\ \left(\frac{Y_j - L_j}{T_j - L_j}\right)^s & if\ L_j \le Y_j \le T_j \\ 1 & if\ Y_j > T_j \end{cases} \tag{12}$$

Desirability function for Y_j response minimization

$$d_j(Y_j) = \begin{cases} 1 & if\ Y_j < T_j \\ \left(\frac{Y_j - U_j}{T_j - U_j}\right)^t & if\ T_j \le Y_j \le U_j \\ 0 & if\ Y_j > U_j \end{cases} \tag{13}$$

where, s = t =1, the desirability function increases linearity towards T_j , for s < 1, t <1 function is convex; s > 1, t > 1 concave.

After calculating the composite desirability, the multivariate gradient decent algorithm has been deployed for optimizing the process [32]. The expression for calculation has been provided in Eq. (14). Repeat the process until it converges, where J is the cost function (here the composite desirability) , θ_m is the mth decision variable or here it is the process parameter, N is number of process parameters and α is learning rate.

$$\theta_m = \theta_m - \alpha \sum_{m=0}^{N} \frac{\partial}{\partial \theta_m} J(\theta_0, \theta_1, \ldots, \theta_N) \tag{14}$$

The composite desirability change with individual objectives is provided in Figure 9. This indicates for satisfying the objectives the print density should be 87.68%, chamber temperature of 50ºC and orientation of XZ.

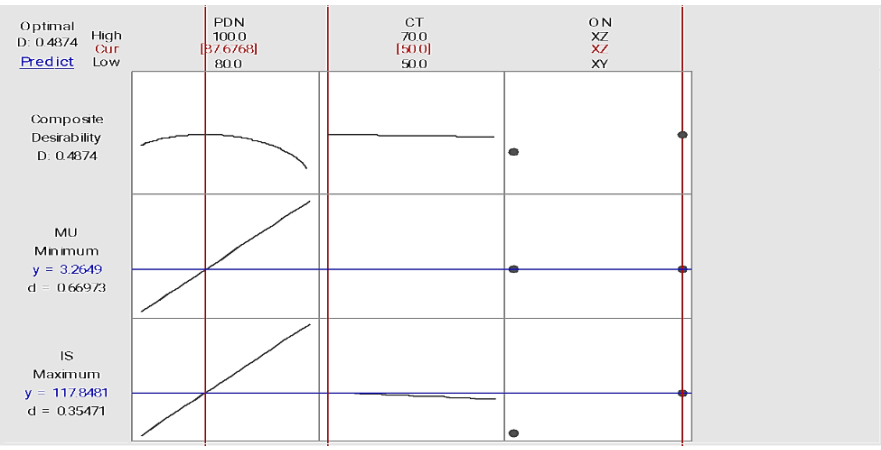

Figure 9. Desirability analysis summary

3.7 Regression Analysis

The Impact Strength estimation model is tried to derive with multiple combinations of process parameters. Regression method is deployed to establish the relationship between the impact strength and process parameters [33]. Here multiple regression models are created and then based on the Akaike Information Criterion (AIC) value [34], tries to find the best fit with minimum number fewest possible independent variable. The multiple fitted models are compared then based on minimum AIC best model is selected. The independent variable here is here impact strength and for improving the model multiple variables are created based on the concept of feature engineering. The variables are ON, PDN, CT, PDN x CT, PDN^2, CT^2. The tested models along with AIC values are provided in Table 17 and a model summary has been provided in Table 18.

Table 17. Model selection for estimating the impact strength

Model	Variable set	AIC
1	ON; PDN; CT; PDN x CT; PDN^2; CT^2	141.58
2	ON; PDN; CT; PDN^2;CT^2	139.60
3	ON; PDN; CT; PDN^2	137.86
4	ON; PDN; PDN^2	135.94
5	ON; PDN^2	135.01

Table 18. The summary of selected impact strength estimation model

	Coefficient	P value	Adjusted R^2
Intercept	-118.6045	0.0418	51.37%
ON: XZ	34.1067	0.0865	
PDN^2	0.0258	0.0010	

The selected predictive model has adjusted R^2 of 51.37%. It is indicating that the model parameters ON and PDN^2 can explain the 51.37% variability within the impact strength. The P value indicates that the PDN^2 have a significant impact on the Impact strength value. Thus, the regression model has been provided as Eq. (15).

$$Impact\ Strength_{XZ=1} = -118.6045 + 34.1067XZ + 0.0258PDN^2 \quad (15)$$

4.0 RESULTS AND DISCUSSION

The three response variables—Impact intensity, Print time, and Material utilization—show that the PDN has the most significance according to the correlation coefficient values and ANOVA. The density of a 3D printed item is the amount of material that fills it up [35]. In general, a higher print density indicates a higher material content and a more robust interior structure. Consequently, printed components with higher PDN values often have better impact resistance. A component with a lower print density could contain holes or weak spots, making it more prone to cracking or breaking upon contact [36]. In contrast, a denser and more solid structure is less likely to do so. It should be noted that although the Print density does impact the quantity of material that has to be deposited and solidified during 3D printing, it is typically the case that higher PDN values result in longer print times since more material needs to be printed. On the other hand, because less material has to be deposited with a lower print density, printing times may be reduced. Nevertheless, it should be mentioned that other variables, including printing technique, layer height, design complexity, etc., may influence the effect on print time. The term "material utilisation" describes how well the 3D printing process makes use of the materials used to make the final product. A decrease in material utilisation efficiency might be the consequence of a higher print density, as it indicates the usage of more material [36]. As less material is needed to accomplish the specified component shape, lower PDN values may result in greater material utilisation. For additive manufacturing to be cost-effective and waste-minimizing, material utilisation efficiency must be maximised [37–39]. It should be noted that the relationship between PDN and the three response variables (impact strength, print time, and material utilisation) may not be linear and can vary further depending on the specific 3D printing technology and object complexity. For more information, see Eq. (15). Previous research has shown a direct relationship between the amount of material used and the amount of time spent printing [38, 39], and there is a perfectly significant positive connection between the two variables. When dealing with three variables, the independent variables of chamber temperature and print orientation do not seem to have a substantial influence. To manage the cooling pace of the produced components or use temperature-sensitive materials like PEEK in FDM, chamber temperature may be a critical variable in certain 3D printing techniques [40, 41]. But by paying close attention to the nozzle temperature during extrusion, we were able to regulate the melting and solidification of the PEEK filament [10,13,16]. In a short amount of time, the extruded material hardens and joins the deposited layer. The bonding process may be unaffected by the chamber temperature since the melting and solidification happen so quickly after each other. Furthermore, it is common for the extruder head to follow overlapping routes when printing, which increases the likelihood of material fusion between successive passes. The 3D printed part's overall strength is enhanced by the excellent bonding between layers made possible by this overlapping design. The printing process also depends on the print orientation, which describes the 3D model's placement on the build platform. Mechanical qualities, printing time, and material utilisation might vary depending on orientation [42, 43]. While print orientation does affect response variables, it may not always have a major impact, particularly when additional optimisations have been made to print density and layer height. More important for material bonding in FDM are the layer height and extrusion parameters, including nozzle temperature and extrusion rate [41]. By fine-tuning these settings, you can minimise the effect of print orientation and chamber temperature on material bonding, resulting in robust interlayer adhesion and bonding [44]. Traditional Taguchi, TOPSIS-based Taguchi, and Composite Desirability Enabled Gradient Decent are the three approaches used to analyse optimisation cases. The optimisation results show that the Taguchi-based approach is unable to use the orthogonal array to generate results. Nevertheless, this approach reveals once again which

parameters are more influencing while going for optimization. It indicates print density with 100%, chamber temperature of 50^0C and print orientation of XZ produces the highest impact strength but it requires higher print time of 98 min. Similar result also found in case of Taguchi based optimization where the target is maximization of impact strength. As the problem is a multi-objective problem, in that context the composite desirability produces moderate results. It selects the print density as 87.70%, chamber temperature of 50^0C and print orientation of XZ. The solution indicates an impact strength value of 86.5 kJ/m^2, print time of 89 min and material utilization of 3.26 gm. The results from different methods are provided in Table 19. The reader can also refer to Table 20 for the main effect plot and signal to noise(S/N) ratio plot. Finally, the regression model proposed in Table 18 can be represented using Eq. (15), which can be used for estimating the impact strength of a 3D printed object printed with PEEK. The proposed predictive model is nonlinear or quadratic in nature and such model is very rare in the published domain.

Table 19. Objective wise selected process parameter value for optimal performance of the process

Method	Objective	PO	PDN (%)	CT (^{0}C)	IS (kJ/m^2)	PT (min)	MU (gm)
Taguchi	Min PT	-	80	-	-	-	-
Taguchi	Max IS	XZ	100	50	230.4	98	3.64
Taguchi	Min MU	-	80	-	-	-	-
TOPSIS Taguchi	All Three	XZ	100	50	230.4	98	3.64
Composite Desirability with gradient decent method	All Three	XZ	87.70	50	86.5	89	3.26

Table 20. Main plot and S/N plot

Method	Objective	Main Effects Plot for Means	Main Effects Plot for SN ratios
Taguchi	Min PT	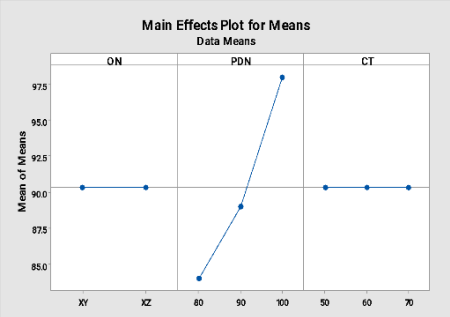	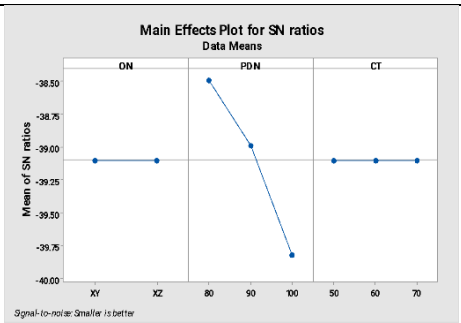
Taguchi	Max IS	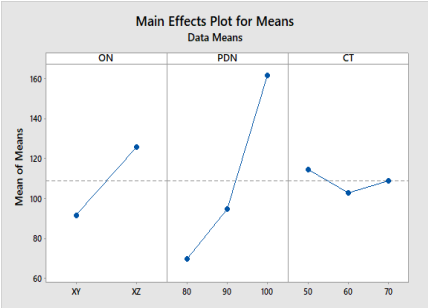	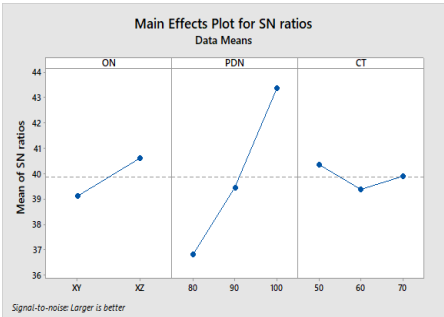
Taguchi	Min MU	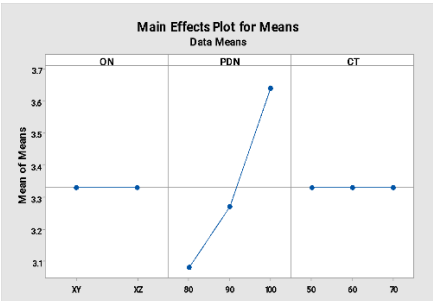	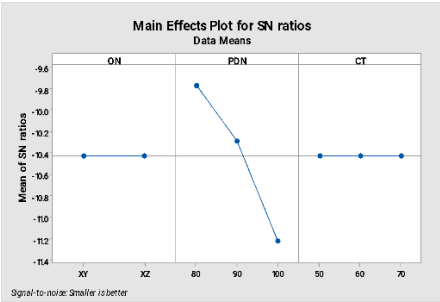

Table 20. (cont.)

Method	Objective	Main Effects Plot for Means	Main Effects Plot for SN ratios
TOPSIS Taguchi	All Three	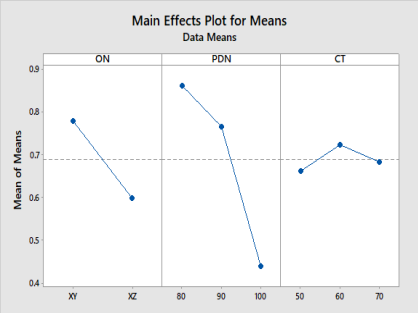	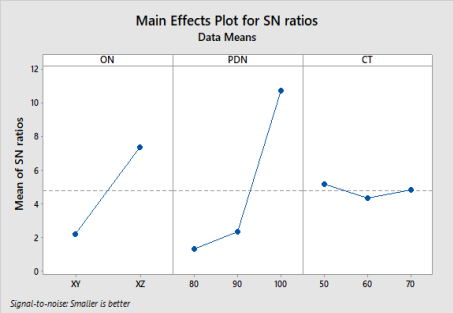

5.0 CONCLUSIONS

The study concludes that higher print density or infill density enhances impact strength of a 3D printed object. However, this increases material usage and print time, which increase the manufacturing cost and time as well. PEEK isa costly printing material and hence, the consideration of material usage in the process optimization added an extra dimension to the problem. The printing time also considered along with the other two response variable for the same process. Finally, the objective of maximization of impact strength, minimization of material usage and minimization of printing time is considered for the process optimization. Different methods are deployed before process optimization to understand the relation between the process parameters and response variables. The correlation analysis and ANOVA indicates that the print density has significant impact on the three response variables. The print time and material usage have full positive significant correlation, which indicates there is a proportional relation between them. On the other side, the impact strength also has positive significant correlation with print time and material usage, which concludes while increasing the impact strength the material usage and printing time is higher. In case of process optimization, the three methods Taguchi, TOPSIS Taguchi and Composite desirability based gradient decent methods are deployed. Taguchi method fails to find the process parameters value for the objectives minimization of print time and material usage but selects the maximum print density of 100%, XZ as print orientation and 50^0C of chamber temperature. Same process parameter values are selected with the TOPSIS based Taguchi method. The Impact strength obtained through is the 230.4kJ/m^2, print time as 98 min and 3.64 gm of material usage. The proposed desirability coupled with gradient decent methodselects print density as 87.70%, XZ as print orientation and 50^0C of chamber temperature. This parameter setup produces Impact strength of 86.5 kJ/m^2, print time of 89 min, whereas 3.26 gm of Material usage, which is close to the treatment no. 13 from L18 OA (see Table 3). This definitely produces a printed object with comparable less impact strength but results in 9.18% less in printing time and 11.66 % of less material usage. Application wise, a minimum and a maximum value range for the impact strength and acceptable range for other response variables can be set for composite desirabilitycoupled gradient decent method for obtaining desired results. Finally, the regression equation for predicting the impact strength has been proposed for the printed material in the XZ plane, which is useful for predicting the impact strength value.

6.0 ACKNOWLEDGMENTS

The authors express their sincere gratitude for the support provided by the Science and Engineering Research Board (SERB), Department of Science and Technology (DST), Government of India, through the Teachers Association for Research Excellence (TARE) scheme (Grant number: TAR/2020/000160).

7.0 REFERENCES

[1] S. Vyavahare, S. Teraiya, D. Panghal and S. Kumar, "Fused deposition modelling: A review," *Rapid Prototyping Journal*, vol. 26, no. 1, pp.176-201, 2020.

[2] L. Sandanamsamy, W. S. W. Harun, I. Ishak, F. R. M. Romlay, K. Kadirgama, D. Ramasamy, S. R. A. Idris and F. Tsumori, "A comprehensive review on fused deposition modelling of polylactic acid," *Progress in Additive Manufacturing*, vol. 8, pp. 775-799, 2023.

[3] S. Sunpreet, P. Chander and R. Seeram, "3D printing of polyether-ether-ketone for biomedical applications," *European Polymer Journal*, vol. 114, pp. 234-248, 2019.

[4] D. Arit, A. C. Camden, J. F. Jacob, E. Z. Callie, L. G. Eric, B. W. Christopher and J. B. Michael, "Current understanding and challenges in high temperature additive manufacturing of engineering thermoplastic polymers," *Additive Manufacturing*, vol. 34, p. 101218, 2020.

[5] D. Garcia-Gonzalez, A. Rusinek, T. Jankowiak, and A. Arias, "Mechanical impact behavior of polyether–ether–ketone (PEEK)," *Composite Structures*, vol. 124, pp. 88-99, 2015.

[6] K. Rajan, M. Samykano, K. Kadirgama, W. S. W. Harun, and M. M. Rahman, "Fused deposition modeling: Process, materials, parameters, properties, and applications," *International Journal of Advanced Manufacturing Technology*, vol. 120, no. 3-4, pp. 1531–1570, 2022.

[7] H. Gonabadi, Y. Chen, A. Yadav, and S. Bull, "Investigation of the effect of raster angle, build orientation, and infill density on the elastic response of 3D printed parts using finite element microstructural modeling and homogenization techniques," *International Journal of Advanced Manufacturing Technology*, vol. 118, pp. 1485–1510, 2022.

[8] A. Murali, M. A. Vakkattil and R. Parameswaran, "Investigating the effect of processing parameters on mechanical behavior of 3D fused deposition modeling printed polylactic acid," *Journal of Material Engineering and Performance*, vol. 32, pp. 1089–1102, 2023.

[9] A. C. Christopher, Í. G. da Silva, K. D. Pangilinan, Q. Chen, E. B. Caldona and R. C. Advincula, "High performance polymers for oil and gas applications," *Reactive and Functional Polymers*, vol. 162, p. 104878, 2021.

[10] Z. Zhang, C. Breidt, L. Chang and K. Friedrich, "Wear of PEEK composites related to their mechanical performances," *Tribology International*, vol. 37, no. 3, pp. 271-277, 2004.

[11] W. Z. Wu, P. Geng, J. Zhao, Y. Zhang, D. W. Rosen and B. H. Zhang, "Manufacture and thermal deformation analysis of semicrystalline polymer polyether ether ketone by 3D printing," *Materials Research Innovations*, vol. 18, no. 5, pp. 12-16, 2014.

[12] C. Yang, X. Tian, D. Li, Y. Cao, F. Zhao and C. Shi, "Influence of thermal processing conditions in 3D printing on the crystallinity and mechanical properties of PEEK material," *Journal of Materials Processing Technology*, vol. 248, pp. 1-7, 2017.

[13] S. Berretta, R. Davies, Y.T. Shyng, Y. Wang and O. Ghita, "Fused deposition modelling of high temperature polymers: Exploring CNT PEEK composites," *Polymer Testing*, vol. 63, pp. 251-262, 2017.

[14] M. Rinaldi, T. Ghidini, F. Cecchini, A. Brandao and F. Nanni, "Additive layer manufacturing of poly (ether ether ketone) via FDM," *Composites Part B*, vol. 145, pp. 162-172, 2018.

[15] X. Deng, Z. Zeng, B. Peng, S. Yan and W. Ke, "Mechanical properties optimization of poly-ether-ether-ketone via fused deposition modeling," *Materials*, vol. 11, no. 2, pp. 216, 2018.

[16] M. F. Arif, S. Kumar, K. M. Varadarajan and W. J. Cantwell, "Performance of biocompatible PEEK processed by fused deposition additive manufacturing," *Materials & Design*, vol. 146, pp. 249-259, 2018.

[17] S. A. Muhsin, P. V. Hatton, A. Johnson, N. Sereno and D. J. Wood, "Determination of Polyetheretherketone (PEEK) mechanical properties as a denture material," *The Saudi Dental Journal*, vol. 31, no. 3, pp. 382-391, 2019.

[18] P. Wang, B. Zou, H. Xiao, S. Ding and C. Huang, "Effects of printing parameters of fused deposition modeling on mechanical properties, surface quality, and microstructure of PEEK," *Journal of Materials Processing Technology*, vol. 271, pp. 62-74, 2019.

[19] Q. Li, W. Zhao, Y. Li, W. Yang, and G. Wang, "Flexural properties and fracture behavior of CF/PEEK in orthogonal building orientation by FDM: Microstructure and mechanism," *Polymers*, vol. 11, no. 4, pp. 656, 2019.

[20] S. Yingshuang, W. Xian, L. Yifan, J. Zilong, W. Zhaoyang, J. Zhenhua and Z. Haibo, "Preparation of PEEK/MWCNTs composites with excellent mechanical and tribological properties," *High Performance Polymers*, vol. 31, no. 1, pp. 43–50, 2019.

[21] G. Haijun, X. Xiaodong and N. Jan, "Impact strength of 3D printed polyether-ether-ketone (PEEK)," in *Proceedings of the 30th Annual International Solid Freeform Fabrication Symposium—An Additive Manufacturing Conference*, Austin, Texas, USA, pp. 12–14, 2019.

[22] S. Singh, C. Prakash and S. Ramakrishna, "3D printing of polyether-ether-ketone for biomedical applications," *European Polymer Journal*, vol. 114, pp. 234-248, 2019.

[23] J. Zheng, J. Kang, C. Sun, C. Yang, L. Wang and D. Li, "Effects of printing path and material components on mechanical properties of 3D-printed polyether-ether-ketone/hydroxyapatite composites," *Journal of the Mechanical Behavior of Biomedical Materials*, vol. 118, p. 104475, 2021.

[24] G. Cicala, A. Latteri, B. Del Curto, A. L. Russo, G. Recca and S. Farè, "Engineering thermoplastics for additive manufacturing: A critical perspective with experimental evidence to support functional applications," *Journal of Applied Biomaterials & Functional Materials*, vol. 15, pp. 10–18, 2017.

[25] C. Padhy, S. Suryakumar, D. Bhattacharjee, R. Reddy, "Parametric analysis of 3D printing (FDM) process parameters on mechanical behaviour of PEEK- A high-grade polymer", *International Interdisciplinary Conference on Energy, Nanotechnology and Internet of Things*, ENT-2023, NIT-Puducherry, India, February 2-4, 2023.

[26] D. C. Montgomery. Design and Analysis of Experiments, 10th Ed. *John Wiley & Sons Inc.*, 2019.

[27] M. Ezekiel. Methods of Correlation Analysis, 2nd Ed. *John Wiley & Sons Inc.*, 1941.

[28] B. Şimşek and T. Uygunoğlu, "Multi-response optimization of polymer blended concrete: A TOPSIS based Taguchi application." *Construction and Building Materials*, vol. 117, pp. 251-262, 2016.

[29] D. Bhattacharjee, T. Ghosh, P. Bhola, K. Martinsen and P. Dan, "Ecodesigning and improving performance of plugin hybrid electric vehicle in rolling terrain through multi-criteria optimisation of powertrain," *Proceedings of the Institution of Mechanical Engineers, Part D: Journal of Automobile Engineering*, vol. 236, no. 5, pp. 1019-1039, 2022.

[30] H. Korucu, B. Şimşek and A. Yartaşı, "A TOPSIS-based Taguchi design to investigate optimum mixture proportions of graphene oxide powder synthesized by hummers method," *Arabian Journal for Science and Engineering*, vol. 43, pp. 6033-6055, 2018.

[31] N. R. Costa, J. Lourenço and Z. L. Pereira, "Desirability function approach: A review and performance evaluation in adverse conditions," *Chemometrics and Intelligent Laboratory Systems*, vol. 107, no. 2, pp. 234-244, 2011.

[32] S. Ruder, "An overview of gradient descent optimization algorithms," *ArXiv*, vol, abs/1609.04747, 2016.

[33] R. J. Freund, W. J. Wilson and P. Sa. Regression Analysis, 2nd Ed. *Academic Press*, 2006.

[34] A. K. Seghouane, "New AIC corrected variants for multivariate linear regression model selection," *IEEE Transactions on Aerospace and Electronic Systems*, vol. 47, no. 2, pp. 1154-1165, 2011.

[35] NWA3D, "Glossary of 3D Printing Terms," *Accessed*: August 2023, Available at https://www.nwa3d.com/education/glossary-of-3d-printing-terms/

[36] J. Dobos, M. M. Hanon and I. Oldal, "Effect of infill density and pattern on the specific load capacity of FDM 3D-printed PLA multi-layer sandwich," *Journal of Polymer Engineering,* vol. 42, no. 2, pp. 118-128, 2022.

[37] I. J. Petrick and T. W. Simpson "3D printing disrupts manufacturing: how economies of one create new rules of competition," *Research-Technology Management*, vol. 56, no. 6 pp. 12–16, 2013.

[38] B. P. Conner, G. P. Manogharan, A. N. Martof, L. M. Rodomsky, C. M. Rodomsky, D. C. Jordan, and J. W. Limperos, "Making sense of 3-D printing: Creating a map of additive manufacturing products and services," *Additive Manufacturing*, vol. 1–4, pp. 64–76, 2014.

[39] B. Liseli, M. Guha, M. Hazel, "Study of infill print design on production cost-time of 3D printed ABS parts," *International Journal of Rapid Manufacturing*, vol. 5, no. 3/4, pp. 308-319, 2015.

[40] S. J. Park, J. E. Lee, J. Park, N. K. Lee, Y. Son and S. H. Park, "High-temperature 3D printing of polyetheretherketone products: Perspective on industrial manufacturing applications of super engineering plastics," *Materials & Design*, vol. 211, p. 110163, 2021.

[41] R. Kumrai-Woodruff and Q. Wang, "Temperature control to increase inter-layer bonding strength in fused deposition modelling" *Proceeding of the ASME 2020 International Design Engineering Technical Conferences and Computers and Information in Engineering Conference*, vol. 6, p. V006T06A002, 2020.

[42] S. Kannan, R. Vezhavendhan, S. Kishore and K. V. Kanumuru, "Investigating the effect of orientation, infill density with Triple raster pattern on the tensile properties for 3D Printed samples," *IOPSciNotes,* vol. 1, p. 024405, 2020.

[43] B. W. Kaplun, R. Zhou, K. W. Jones, M. L. Dunn and C. M. Yakacki, "Influence of orientation on mechanical properties for high-performance fused filament fabricated ultem 9085 and electro-statically dissipative polyetherketoneketone," *Additive Manufacturing*, vol. 36, p. 101527, 2020.

[44] O. A. Mohamed, S. H. Masood and J. L. Bhowmik. "Optimization of fused deposition modeling process parameters: A review of current research and future prospects," *Advances in Manufacturing*, vol. 3, pp. 42-53, 2015.